物理学报 Acta Physica Sinica
Chinese Physical Society
Institute of Physics, CAS

随机电磁光束经像散透镜后磁场的光谱Stokes奇点

郑尚彬 唐碧华 姜云海 高曾辉 罗亚梅

Magnetic spectral Stokes singularities of stochastic electromagnetic beams through an astigmatic lens

Zheng Shang-Bin Tang Bi-Hua Jiang Yun-Hai Gao Zeng-Hui Luo Ya-Mei

引用信息 Citation: Acta Physica Sinica, 65, 234201 (2016) DOI: 10.7498/aps.65.234201
在线阅读 View online: http://dx.doi.org/10.7498/aps.65.234201
当期内容 View table of contents: http://wulixb.iphy.ac.cn/CN/Y2016/V65/I23

随机电磁光束经像散透镜后磁场的光谱Stokes奇点*

郑尚彬[1)] 唐碧华[1)] 姜云海[1)] 高曾辉[2)] 罗亚梅[1)2)†]

1)(西南医科大学医学信息与工程学院, 泸州 646000)

2)(宜宾学院, 计算物理重点实验室, 宜宾 644000)

(2016年5月16日收到; 2016年9月8日收到修改稿)

利用交叉谱密度函数的传输公式, 以部分相干刃型位错光束为例, 推导出随机电磁光束磁场通过像散透镜传输后的解析表达式. 使用光谱Stokes参数, 详细讨论了光谱Stokes场的奇点变化规律. 结果表明, 随机电磁光束磁场通过透镜后的传输过程中, 存在光谱s_{12}, s_{23}和s_{31}奇点. 改变刃型位错的离轴量、斜率、空间相关长度等光束参数以及随着传输距离的变化, 会有磁场光谱Stokes奇点的移动、产生和湮没, 也会有V点的产生和C点旋向性的反转. 此外, 还与电场的光谱Stokes奇点做了比较.

关键词: 随机电磁光束, 像散透镜, 磁场光谱Stokes奇点

PACS: 42.25.Bs, 42.25.Ja **DOI:** 10.7498/aps.65.234201

1 引 言

自Nye发现矢量场具有偏振奇点后, 对偏振奇点已做了广泛的理论和实验研究[1−26], 并基于此提出了奇异偏振术, 这一新技术在亚微米粒子的变形和位移精确测量以及生命科学研究中得到应用. 对于偏振奇点, 可以使用电磁场理论或Stokes参数来分析[3,14], 也可以用复Stokes场描述[6,8,12,15]. 在某些实际应用中, 部分相干光比完全相干光更具优越性[27], 例如, 部分相干光在大气中传输时受大气扰动的影响要比完全相干光小得多, 从而使得部分相干光能更好地应用于光通信中. 近来, 对于偏振奇点的研究对象已从完全相干光扩展到部分相干光, Yan和Lü[18]通过引入Korotkova和Wolf提出的光谱Stokes参数, 将完全相干光的偏振奇点推广到部分相干光, 讨论了自由空间中的光谱Stokes奇点. Luo和Lü[22]研究了非傍轴部分相干涡旋光束叠加场在自由空间中传输的合成光谱Stokes奇点的演化特性. 此外, Hajnal[23]通过实验研究了微波在自由空间传输过程中三维电场和磁场的偏振奇点, 证实了一般情况下的电场和磁场的偏振奇点并不相同. Berry[24]则对矢量波的横向场(二维)以及三维电场和磁场偏振奇点做了比较研究. Luo等[25,26]研究了高斯涡旋光束在自由空间和聚焦空间, 二维和三维电场和磁场的偏振奇点在自由空间和焦区的移动、产生和湮没等现象. 本文以部分相干刃型位错光束为例, 对随机电磁光束磁场经像散透镜后的光谱Stokes奇点演化特性做了详细研究, 并与电场的光谱Stokes奇点做了比较.

2 理论模型

设$z=0$面处的刃型位错光束的电场分量表示为:

$$E_x(x_0,y_0,0) = A_x\left(\frac{a_x x_0+y_0+d_x}{w_0}\right)\exp\left[-\frac{x_0^2+y_0^2}{w_0^2}\right], \quad (1a)$$

* 国家自然科学基金(批准号: 61275203, 61505075)和四川省教育厅自然科学基金(批准号: 15CZ0017)资助的课题.

† 通信作者. E-mail: luoluoeryan@126.com

$$E_y(x_0,y_0,0) = A_y\left(\frac{a_y x_0+y_0+d_y}{w_0}\right)\exp\left[-\frac{x_0^2+y_0^2}{w_0^2}\right], \quad (1b)$$

其中, $(x_0,\ y_0)$ 是 $z=0$ 平面处的位置坐标, A_x, A_y 分别是 E_x 和 E_y 的振幅常量, w_0 为束腰宽度, d_x 和 d_y, a_x 和 a_y 是分别寄居于 E_x 和 E_y 分量中的刃型位错的离轴距离及斜率.

在傍轴近似下, 对应于电场 E_x, E_y 的磁场分量为[24]:

$$B_x(x_0,y_0,0) = -\frac{1}{c}E_y(x_0,y_0,0), \quad (2a)$$

$$B_y(x_0,y_0,0) = \frac{1}{c}E_x(x_0,y_0,0), \quad (2b)$$

其中, c 为真空中的光速.

部分相干光光场在空间-频率域内, 可用任意两点 (r_1,r_2) 的交叉谱密度矩阵 $\boldsymbol{W}(r_1,\ r_2)$ 来描述[21,28]. 根据定义可得在 $z=0$ 处, 随机电磁光束磁场交叉谱密度矩阵表示为

$$\boldsymbol{W}_{uv}(x_{01},y_{01},x_{02},y_{02},0) = \langle B_u^*(x_{01},y_{01},0)B_v(x_{02},y_{02},0)\rangle, \quad (3)$$

式中 $\langle\ \rangle$ 表示系综平均, $*$ 表示复共轭, u, v=x, y. 把 (1) 式和 (2) 式代入 (3) 式, 考虑谢尔模型光束, 则其交叉谱密度矩阵元在 $z=0$ 面表示为:

$$W_{xx}(x_{01},y_{01},x_{02},y_{02},0) = \frac{1}{c^2}\frac{A_yA_y}{w_0w_0}C_{xx}(a_yx_{01}+y_{01}+d_y)(a_yx_{02}+y_{02}+d_y)\exp\left(-\frac{x_{01}^2+y_{01}^2}{w_0^2}\right)\exp\left(-\frac{x_{02}^2+y_{02}^2}{w_0^2}\right)\exp\left[-\frac{(x_{01}-x_{02})^2+(y_{01}-y_{02})^2}{2\delta_{xx}^2}\right], \quad (4a)$$

$$W_{yy}(x_{01},y_{01},x_{02},y_{02},0) = \frac{1}{c^2}\frac{A_xA_x}{w_0w_0}C_{yy}(a_xx_{01}+y_{01}+d_x)(a_xx_{02}+y_{02}+d_x)\exp\left(-\frac{x_{01}^2+y_{01}^2}{w_0^2}\right)\exp\left(-\frac{x_{02}^2+y_{02}^2}{w_0^2}\right)\exp\left[-\frac{(x_{01}-x_{02})^2+(y_{01}-y_{02})^2}{2\delta_{yy}^2}\right], \quad (4b)$$

$$W_{xy}(x_{01},y_{01},x_{02},y_{02},0) = -\frac{1}{c^2}\frac{A_yA_x}{w_0w_0}C_{xy}(a_yx_{01}+y_{01}+d_y)(a_xx_{02}+y_{02}+d_x)\exp\left(-\frac{x_{01}^2+y_{01}^2}{w_0^2}\right)\exp\left(-\frac{x_{02}^2+y_{02}^2}{w_0^2}\right)\exp\left[-\frac{(x_{01}-x_{02})^2+(y_{01}-y_{02})^2}{2\delta_{xy}^2}\right], \quad (4c)$$

$$W_{yx}(x_{01},y_{01},x_{02},y_{02},0) = W_{xy}^*(x_{01},y_{01},x_{02},y_{02},0), \quad (4d)$$

其中, 式中 $C_{uv}=C_{vu}^*$, 一般情况下当 $u\neq v$ 时是复数, 而当 $u=v$ 时, $C_{uv}=1$; δ_{uv} 为部分相关长度.

假设光束经过一焦距为 f, 位于 $z=0$ 面处的像散透镜聚焦, 利用交叉谱密度通过像散透镜的传输公式[28], z 处的交叉谱密度矩阵元表示为

$$\begin{aligned}W_{uv}(x_1,y_1,x_2,y_2,z) = {}& \left(\frac{k}{2\pi z}\right)^2\exp\left[-\mathrm{i}\frac{k}{2z}(x_1^2+y_1^2-x_2^2-y_2^2)\right]\\ &\times\iiiint W_{uv}(x_{01},y_{01},x_{02},y_{02},0)\\ &\times\exp\left[-\mathrm{i}\frac{k}{2z}\left(1-\frac{z}{f}\right)(x_{01}^2+y_{01}^2-x_{02}^2-y_{02}^2)\right]\\ &\times\exp\left[\mathrm{i}kC_6(x_{01}^2-x_{02}^2-y_{01}^2+y_{02}^2)\right.\\ &\left.+\mathrm{i}\frac{k}{z}(x_1x_{01}+y_1y_{01}-x_2x_{02}-y_2y_{02})\right]\\ &\times\mathrm{d}x_{01}\mathrm{d}y_{01}\mathrm{d}x_{02}\mathrm{d}y_{02},\end{aligned} \quad (5)$$

其中 $(x_1,\ y_1)$, $(x_2,\ y_2)$ 是 z 平面处两点的位置坐标, k 是与波长 λ 有关的波数且 $k=2\pi/\lambda$, C_6 为透镜的像散系数. 把 (4a)—(4d) 式代入 (5) 式, 并令 $x_1=x_2=x$, $y_1=y_2=y$, 经过积分得到:

$$W_{xx}(x,y,z) = \frac{1}{c^2}\frac{A_y^2}{w_0^2}C_{xx}\left(\frac{k}{2w_0z}\right)^2\frac{1}{\sqrt{\alpha_{xx1}\alpha_{xx2}p_{xx1}p_{xx2}}}\left[\frac{1+\dfrac{2q_{xx2}^2}{p_{xx2}}}{4\delta_{xx}^2\alpha_{xx2}p_{xx2}}+\frac{h_{xx}q_{xx2}}{p_{xx2}}+\beta_{xx}\right]\exp\left[\frac{q_{xx1}^2}{p_{xx1}}+\frac{q_{xx2}^2}{p_{xx2}}-\frac{k^2x^2}{4z^2\alpha_{xx1}}-\frac{k^2y^2}{4z^2\alpha_{xx2}}\right], \quad (6a)$$

$$W_{yy}(x,y,z) = \frac{1}{c^2}\frac{A_x^2}{w_0^2}C_{yy}\left(\frac{k}{2w_0z}\right)^2\frac{1}{\sqrt{\alpha_{yy1}\alpha_{yy2}p_{yy1}p_{yy2}}}$$

$$\times\left[\frac{1+\dfrac{2q_{yy2}^2}{p_{yy2}}}{4\delta_{yy}^2\alpha_{yy2}p_{yy2}}+\frac{h_{yy}q_{yy2}}{p_{yy2}}+\beta_{yy}\right]\times\exp\left[\frac{q_{yy1}^2}{p_{yy1}}+\frac{q_{yy2}^2}{p_{yy2}}-\frac{k^2x^2}{4z^2\alpha_{yy1}}-\frac{k^2y^2}{4z^2\alpha_{yy2}}\right], \tag{6b}$$

$$W_{xy}(x,y,z) = -\frac{1}{c^2}\frac{A_xA_y}{w_0^2}C_{xy}\left(\frac{k}{2w_0z}\right)^2\frac{1}{\sqrt{\alpha_{xy1}\alpha_{xy2}p_{xy1}p_{xy2}}}\times\left[\frac{1+\dfrac{2q_{xy2}^2}{p_{xy2}}}{4\delta_{xy}^2\alpha_{xy2}p_{xy2}}+\frac{h_{xy}q_{xy2}}{p_{xy2}}+\beta_{xy}\right]\times\exp\left[\frac{q_{xy1}^2}{p_{xy1}}+\frac{q_{xy2}^2}{p_{xy2}}-\frac{k^2x^2}{4z^2\alpha_{xy1}}-\frac{k^2y^2}{4z^2\alpha_{xy2}}\right], \tag{6c}$$

$$W_{yx}(x,y,z) = W_{xy}^*(x,y,z), \tag{6d}$$

其中

$$\alpha_{uv1} = \frac{1}{w_0^2}+\frac{\mathrm{i}k}{2z}\left(1-\frac{z}{f}\right)+\frac{1}{2\delta_{uv}^2}-\mathrm{i}kC_6,$$

$$\alpha_{uv2} = \frac{1}{w_0^2}+\frac{\mathrm{i}k}{2z}\left(1-\frac{z}{f}\right)+\frac{1}{2\delta_{uv}^2}+\mathrm{i}kC_6,$$

$$p_{uv1} = \frac{1}{w_0^2}+\frac{1}{2\delta_{uv}^2}-\frac{\mathrm{i}k}{2z}\left(1-\frac{z}{f}\right)-\frac{1}{4\delta_{uv}^2\alpha_{uv1}}+\mathrm{i}kC_6,$$

$$p_{uv2} = \frac{1}{w_0^2}+\frac{1}{2\delta_{uv}^2}-\frac{\mathrm{i}k}{2z}\left(1-\frac{z}{f}\right)-\frac{1}{4\delta_{uv}^2\alpha_{uv2}}-\mathrm{i}kC_6,$$

$$q_{uv1} = \frac{\mathrm{i}kx}{2z}\left(\frac{1}{2\delta_{uv}^2\alpha_{uv1}}-1\right),$$

$$q_{uv2} = \frac{\mathrm{i}ky}{2z}\left(\frac{1}{2\delta_{uv}^2\alpha_{uv2}}-1\right),$$

$$h_{xx} = -\frac{q_{xx1}}{2\delta_{xx}^2p_{xx1}}\left(\frac{a_y}{\alpha_{xx1}}+\frac{a_y}{\alpha_{xx2}}\right)-\frac{d_y}{2\alpha_{xx2}\delta_{xx}^2}+\frac{\mathrm{i}ky}{2z\alpha_{xx2}}-\left(\frac{\mathrm{i}kxa_y}{2z\alpha_{xx1}}+d_y\right),$$

$$h_{yy} = -\frac{q_{yy1}}{2\delta_{yy}^2p_{yy1}}\left(\frac{a_x}{\alpha_{yy1}}+\frac{a_x}{\alpha_{yy2}}\right)-\frac{d_x}{2\alpha_{yy2}\delta_{yy}^2}+\frac{\mathrm{i}ky}{2z\alpha_{yy2}}-\left(\frac{\mathrm{i}kxa_x}{2z\alpha_{yy1}}+d_x\right),$$

$$h_{xy} = -\frac{q_{xy1}}{2\delta_{xy}^2p_{xy1}}\left(\frac{a_y}{\alpha_{xy1}}+\frac{a_x}{\alpha_{xy2}}\right)-\frac{a_xq_{xy1}}{2\delta_{xy}^2\alpha_{xy1}p_{xy2}}-\frac{d_x}{2\alpha_{xy2}\delta_{xy}^2}+\frac{\mathrm{i}ky}{2z\alpha_{xy2}}-\left(\frac{\mathrm{i}kxa_y}{2z\alpha_{xy1}}+d_y\right),$$

$$\beta_{xx} = \frac{a_y^2}{4\delta_{xx}^2\alpha_{xx1}p_{xx1}}\left(1+\frac{2q_{xx1}^2}{p_{xx1}}\right)-\frac{\mathrm{i}kyd_y}{2z\alpha_{xx2}}+d_y\left(\frac{\mathrm{i}kxa_y}{2z\alpha_{xx1}}+d_y\right)+\frac{q_{xx1}}{p_{xx1}}\left(-\frac{\mathrm{i}kya_y}{2z\alpha_{xx2}}+a_yd_y+\frac{\mathrm{i}kxa_y^2}{2z\alpha_{xx1}}+\frac{a_yd_y}{2\delta_{xx}^2\alpha_{xx1}}\right),$$

$$\beta_{yy} = \frac{a_x^2}{4\delta_{yy}^2\alpha_{yy1}p_{yy1}}\left(1+\frac{2q_{yy1}^2}{p_{yy1}}\right)-\frac{\mathrm{i}kyd_x}{2z\alpha_{yy2}}+d_y\left(\frac{\mathrm{i}kxa_x}{2z\alpha_{yy1}}+d_x\right)+\frac{q_{yy1}}{p_{yy1}}\left(-\frac{\mathrm{i}kya_x}{2z\alpha_{yy2}}+a_xd_x+\frac{\mathrm{i}kxa_x^2}{2z\alpha_{yy1}}+\frac{a_xd_x}{2\delta_{yy}^2\alpha_{yy1}}\right),$$

$$\beta_{xy} = \frac{a_xa_y}{4\delta_{xy}^2\alpha_{xy1}p_{xy1}}\left(1+\frac{2q_{xy1}^2}{p_{xy1}}\right)-\frac{\mathrm{i}kyd_x}{2z\alpha_{xy2}}+d_x\left(\frac{\mathrm{i}kxa_y}{2z\alpha_{xy1}}+d_y\right)+\frac{q_{xy1}}{p_{xy1}}\left(-\frac{\mathrm{i}kya_x}{2z\alpha_{xy2}}+a_xd_y+\frac{\mathrm{i}kxa_ya_x}{2z\alpha_{xy1}}+\frac{a_yd_x}{2\delta_{xy}^2\alpha_{xy1}}\right).$$

光谱 Stokes 参数定义为[21]

$$S_0(x,y,z) = W_{xx}(x,y,z)+W_{yy}(x,y,z), \tag{7a}$$

$$S_1(x,y,z) = W_{xx}(x,y,z)-W_{yy}(x,y,z), \tag{7b}$$

$$S_2(x,y,z) = W_{xy}(x,y,z)+W_{yx}(x,y,z), \tag{7c}$$

$$S_3(x,y,z) = \mathrm{i}[W_{yx}(x,y,z)-W_{xy}(x,y,z)]. \tag{7d}$$

归一化的谱 Stokes 参数为 $s_1 = S_1/S_0$, $s_2 = S_2/S_0$ 和 $s_3 = S_3/S_0$.

复光谱 Stokes 场 s_{ij} (i, j = 1, 2, 3, 除非特别说明) 为

$$s_{12} = s_1+\mathrm{i}s_2, \tag{8a}$$

$$s_{23} = s_2+\mathrm{i}s_3, \tag{8b}$$

$$s_{31} = s_3+\mathrm{i}s_1, \tag{8c}$$

将 (6) 式代入 (7) 式和 (8) 式, 可得归一化光谱 Stokes 参数和复光谱 Stokes 场的解析结果. 光谱 Stokes 奇点对应于复光谱 Stokes 场 $s_{ij} = 0$, 即 (8a)—(8c) 式的零值点 (或位相奇点). s_{12} 奇点对应于随机电磁束磁场的 C 点, 退化为圆偏振, $s_3 > 0$ ($s_3 < 0$) 对应该点的右旋 (左旋) 性. s_{23} 和 s_{31} 光谱奇点都处于 L 线上, 在该线上的所有点的旋向性不确定, 都为线偏振点[18]. 由 (6)—(8) 式可以看出, 部分相干刃型位错光束的光谱 Stokes 奇点随光束的刃型位错的离轴量、斜率、空间相关长度、透镜的像散系数等控制参数, 以及传输距离 z 变化.

3 磁场光谱Stokes奇点随光束控制参数的变化

3.1 磁场光谱Stokes奇点随刃型位错斜率的变化

根据(8a)—(8c)式, 图1给出了 $z = 0.9f$ 处不同刃型位错离轴量 d_x 时磁场的 $s_1 = 0$(实线), $s_2 = 0$(虚线)和 $s_3 = 0$(点线, 也即 L 线)的等值线分布图. 参数取值为 $C_{xx} = C_{yy} = 1$, $C_{xy} = \exp(\mathrm{i}\pi/3)$, $A_x = 1$, $A_y = 1.5$, $w_0 = 1$ mm, $\lambda = 632.8$ nm, $\delta_{xx} = \delta_{yy} = 0.225$ mm, $\delta_{xy} = \delta_{yx} = 0.225$ mm, $a_x = 0.9$, $a_y = 0.95$, $d_y = -0.45$ mm, $f = 200$ mm, $C_6 = 0.5 \times 10^{-3}$ mm^{-1}, 刃型位错离轴量 d_x 分别为(a) $d_x = 0.24$ mm, (b) $d_x = 0.15$ mm, (c) $d_x = 0.08$ mm, (d) $d_x = 0.01$ mm, (e) $d_x = -0.30$ mm. 图中, 实线与虚线的交点为磁场光谱 s_{12} 奇点, 即磁场 C 点, "○"代表拓扑电荷 $m = +1$ 的 C 点, "●"代表拓扑电荷 $m = -1$ 的 C 点; 虚线与点线的交点为磁场光谱 s_{23} 奇点, "△"代表拓扑电荷 $m = +1$ 的光谱 s_{23} 奇点, "▲"代表拓扑电荷 $m = -1$ 的光谱 s_{23} 奇点; 实线与点线的交点为磁场光谱 s_{31} 奇点, "□"代表拓扑电荷 $m = +1$ 的光谱 s_{31} 奇点, "■"代表拓扑电荷 $m = -1$ 的光谱 s_{31} 奇点(拓扑电荷的值由符号法则决定[29]). 图中 $s_3 = 0$ 等值线, 即 L 线是左旋和右旋区域的分界线[14], "+"号表示的区域为右旋区域, "−"号表示的区域为左旋区域.

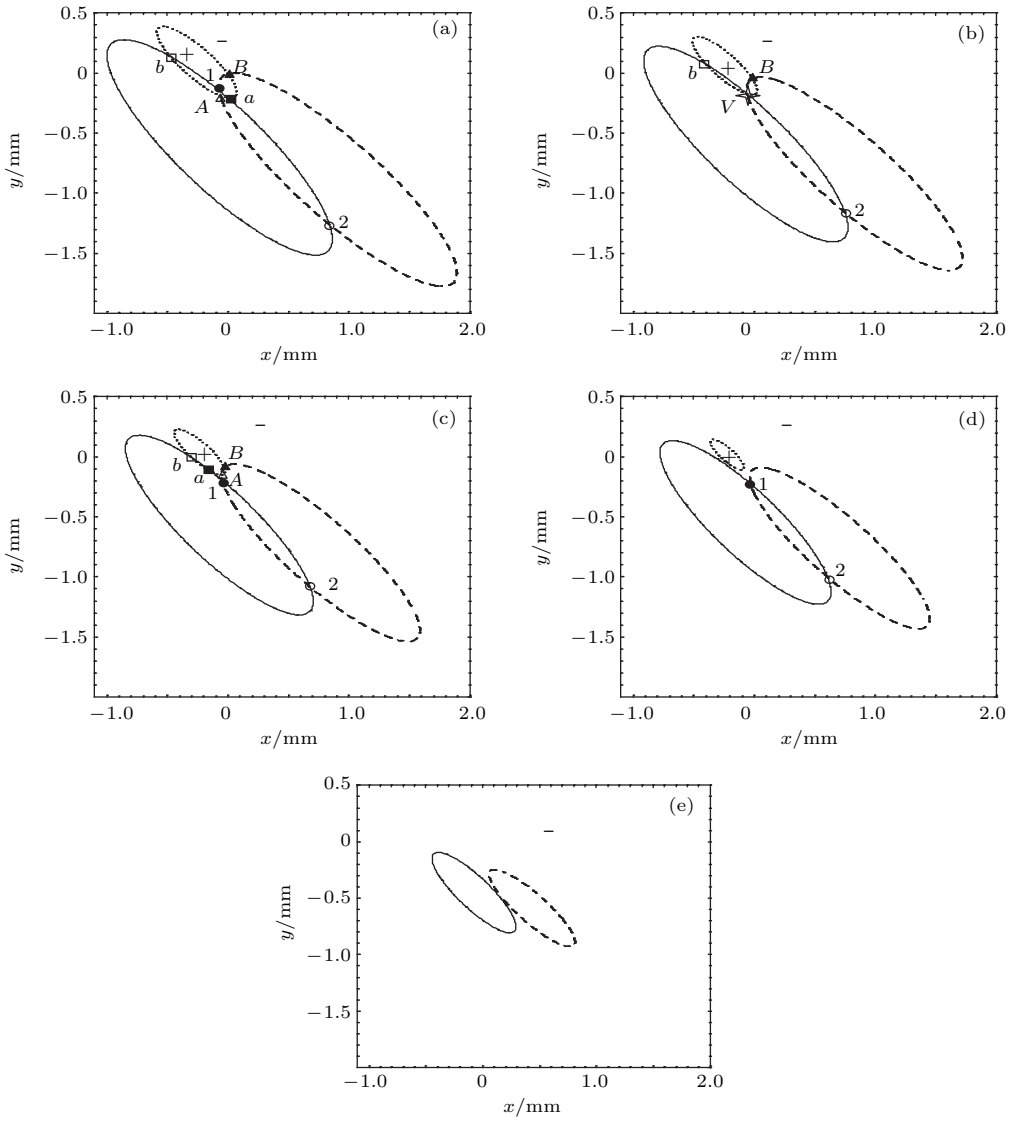

图1 不同离轴量时磁场 $s_1 = 0$, $s_2 = 0$ 和 $s_3 = 0$ 的等值线分布图

Fig. 1. Contour lines of $s_1 = 0$, $s_2 = 0$ and $s_3 = 0$ for different values of the off-axis distance in magnetic field.

由图1可见, 当刃型位错离轴量$d_x = 0.24$ mm时, 在$\{-1.1\ \text{mm} \leqslant x \leqslant 2.0\ \text{mm},\ -2.0\ \text{mm} \leqslant y \leqslant 0.5\ \text{mm}\}$范围内有一个右旋$C$点1和一个左旋$C$点2 (见图1(a)), 位置$(x/\text{mm},\ y/\text{mm})$分别为$1(-0.074, -0.142)$和$2(0.842, -1.263)$. 各$C$点的拓扑电荷为$m_1 = -1$, $m_2 = +1$. 随着刃型位错离轴量的变化, 各C点有所移动并有旋向性反转和湮没现象的出现. 例如$d_x = 0.15$ mm时(见图1(b)), C点1与L线碰撞在一起, 或者说C点1, 光谱s_{23}奇点A, 光谱s_{31}奇点a三类奇点重合于点$(-0.059, -0.171)$处, 出现一个V点(即矢量奇点), 该点的偏振度为0, 偏振态不确定[14]. C点2则移至$2(0.752, -1.165)$. 而当d_x继续减小, 例如$d_x = 0.08$ mm时(见图1(c)), C点$1(-0.047, -0.195)$已处于L线的另一侧, 即其旋向性发生反转, 变为左旋C点, 而C点2仍然为左旋, 位于$(0.681, -1.086)$. 若继续减小d_x, 拓扑电荷相反但同为左旋的两个C点会互相靠近直至湮没. 当$d_x = 0.01$ mm时(见图1(d)), C点1和2分别位于$1(-0.032, -0.222)$, $2(0.608, -1.005)$. 当$d_x = -0.30$ mm时(见图1(e)), 两个C点已经湮没.

当$d_x = 0.24$ mm时, 在$\{-1.1\ \text{mm} \leqslant x \leqslant 2.0\ \text{mm},\ -2.0\ \text{mm} \leqslant y \leqslant 0.5\ \text{mm}\}$范围内有两个光谱$s_{23}$奇点$A$和$B$ (见图1(a)), 位置$(x/\text{mm},\ y/\text{mm})$分别为$A(-0.064, -0.188)$和$B(-0.002,\ -0.005)$, 且拓扑电荷为$m_A = +1$, $m_B = -1$. 随着刃型位错离轴量的变化, 光谱s_{23}奇点A和B有所移动而靠拢, 最终湮没. 例如减小至$d_x = 0.08$ mm (见图1(c)), 光谱s_{23}奇点A和B已移至$A(-0.052, -0.151)$, $B(-0.030,\ -0.088)$. 当$d_x = 0.01$ mm (见图1(d))时, 这对拓扑电荷相反的光谱s_{23}奇点A和B已湮没.

同时, 当$d_x = 0.24$ mm时, 在$\{-1.1\ \text{mm} \leqslant x \leqslant 2.0\ \text{mm},\ -2.0\ \text{mm} \leqslant y \leqslant 0.5\ \text{mm}\}$范围内有两个光谱$s_{31}$奇点$a$和$b$ (见图1(a)), 位置$(x/\text{mm},\ y/\text{mm})$分别为$a(0.334, -0.207)$和$b(-0.484, 0.145)$, 且其拓扑电荷为$m_a = -1$, $m_b = +1$. 若继续变化刃型位错的斜率, 光谱s_{31}奇点也会有所移动并有产生或湮没现象的出现. 例如减小至$d_x = 0.08$ mm (见图1(c)), 光谱s_{23}奇点a和b已移至$a(-0.125, -0.131)$, $b(-0.312, 0.003)$. 当$d_x = 0.01$ mm (见图1(d))时, 这对拓扑电荷相反的光谱s_{31}奇点a和b已湮没.

3.2 磁场光谱Stokes奇点随像散系数的变化

以C点为例, 讨论透镜的像散系数对磁场光谱Stokes奇点的影响. 图2给出了$z = 0.9f$处不同像散系数C_6时磁场的$s_1 = 0$ (实线), $s_2 = 0$ (虚线)的等值线分布图. 透镜的像散参数分别为(a) $C_6 = 0.50 \times 10^{-3}$ mm^{-1}, (b) $C_6 = 0.46 \times 10^{-3}$ mm^{-1}, (c) $C_6 = 0.40 \times 10^{-3}$ mm^{-1}, $d_x = -0.25$ mm, 其余参数同图1. 随着像散系数的变化, 各C点有所

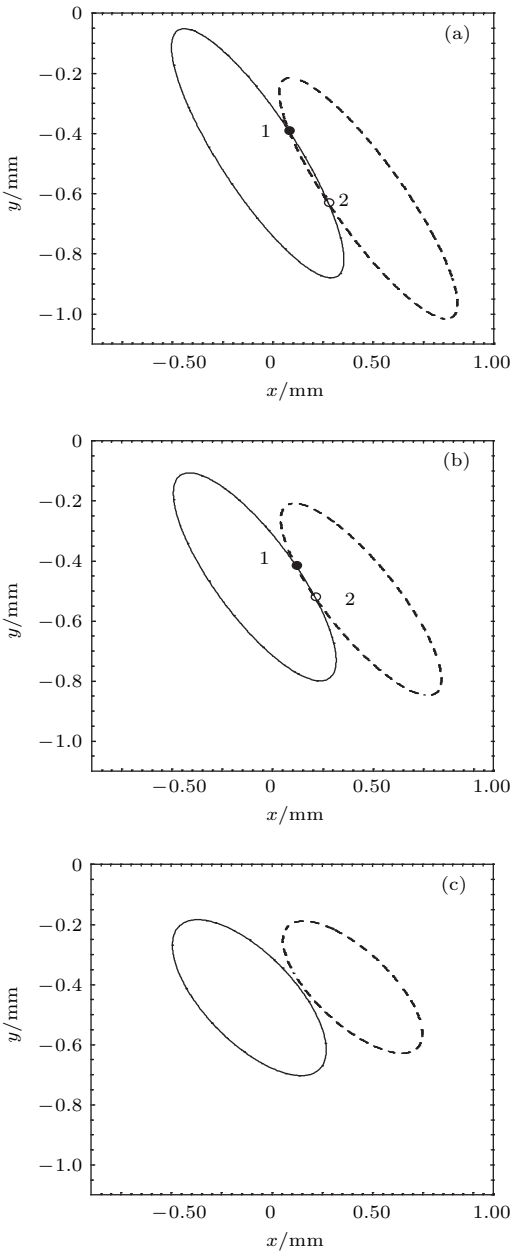

图2 不同透镜像散系数时磁场C点的变化

Fig. 2. Variation of C-points for different values of the astigmatic coefficient in magnetic field.

移动, 并可能湮没. 例如, 当$C_6=0.50\times10^{-3}$ mm^{-1}时(见图2(a)), C点位于1(0.077, −0.388), 2(0.281, −0.637). 而当C_6继续减小至$C_6=0.46\times10^{-3}$ mm^{-1}时(见图2(b)), 两点已更为靠近, 分别位于C点1(0.083, −0.371), 2(0.220, −0.531). 当$C_6=0.40\times10^{-3}$ mm^{-1}时(见图2(c)), 两个C点已经湮没.

类似地, 随着像散系数的变化, s_{23}奇点和s_{31}奇点也有类似规律, 故略去. 当然, 光束的部分相关长度变化也会导致各磁场光谱Stokes奇点产生类似变化, 也略去.

4 磁场光谱Stokes奇点在聚焦空间中的演化

以C点为例, 讨论磁场光谱Stokes奇点在聚焦空间传输过程中的演化. 图3给出了不同传输距离z处的$s_1=0$(实线), $s_2=0$(虚线)的等值线分布图. 参数取值为(a) $z=0.84f$, (b) $z=1.10f$, (c) $z=1.15f$, 其余参数同图2(a). 随着光束在聚焦空间的传输, 会有C点的产生、移动和湮没. 例如, 当$z=0.84f$时(见图3(a)), 在{−0.9 mm $\leqslant x\leqslant$ 1.1 m, −1.1 mm $\leqslant y\leqslant$ 0 mm}范围内没有C点的存在. 当传输至$z=0.90f$时(见图2 (a)), 产生了一对拓扑电荷相反的左旋C点1和2. 随着光束的继续传输, 两个C点相互靠近, 当传输至$z=1.10f$时(见图3(b)), 移至1(−0.062, −0.343), 2(0.072, −0.530). 当传输至$z=1.15f$ (见图3(c)), 两个C点已经湮没.

类似地, 光谱s_{23}奇点A和B以及s_{31}奇点对a和b随传输距离的变化也会有移动、产生和湮没, 故从略.

4.1 与电场光谱Stokes奇点的比较

同样地, 由(1)式出发, 可推导出相应的随机电磁光束电场通过像散透镜传输后的解析表达式(因公式方法类似, 故略去), 用以讨论电场的光谱Stokes场的奇点变化规律. 图4给出了$z=0.90f$时相应电场的$s_1=0$(实线), $s_2=0$(虚线)和$s_3=0$(点线, 也即L线)的等值线分布图, 参数取值与对应图1(a)相同. 由图4可见, 在{−1.1 mm $\leqslant x\leqslant$ 2.0 mm, −2.0 mm $\leqslant y\leqslant$ 0.5 mm}范围内有一个左旋C点1和一个右旋C点2, 位置$(x/\text{mm}, y/\text{mm})$分别为1(−0.034, −0.176)和2(−0.912, 0.272), 且其拓扑电荷为$m_1=+1$, $m_2=-1$. 该范围内也有两个光谱s_{23}奇点A和B, 位置$(x/\text{mm}, y/\text{mm})$分别为$A$(−0.064, −0.188)和$B$(−0.002, −0.005), 且拓扑电荷为$m_A=-1$, $m_B=+1$. 此外, 两个光谱s_{31}奇点a和b的位置$(x/\text{mm}, y/\text{mm})$分别为$a$(−0.106, −0.116)和$b$(0.437, −0.636), 且其拓扑电荷为$m_a=+1$, $m_b=-1$. 和磁场的相应光谱Stokes奇点相比较, 二者的位置、旋向性、拓扑电荷一般并不相同, 且其左右旋区域也是不重合的. 同样地, 随着光束控制参数和传输距离的变化, 各电场光谱Stokes奇点和磁场的变化规律类似, 有所移动并伴随有湮没或产生, 略去.

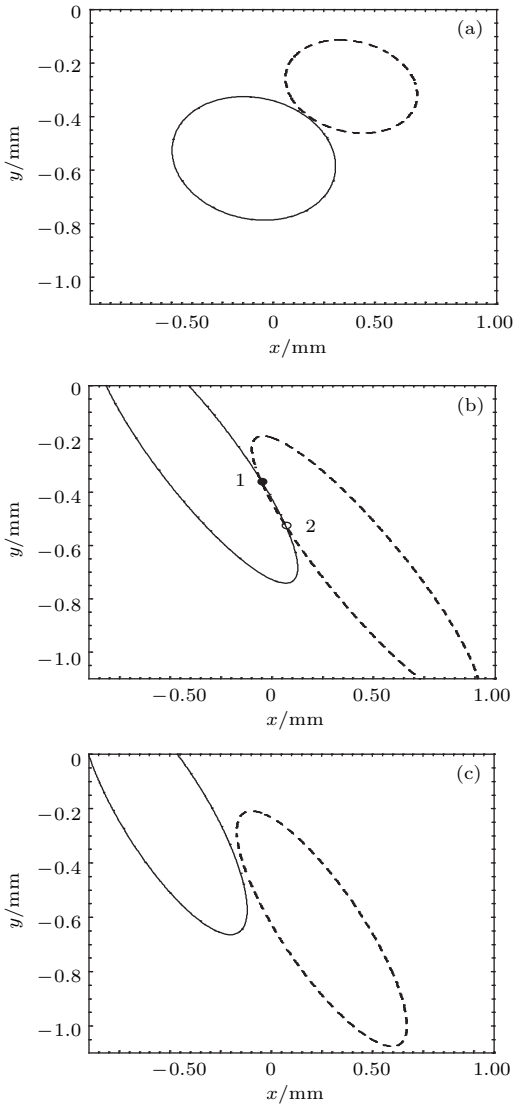

图3 不同传输距离时磁场C点的变化

Fig. 3. Variation of C-points for different values of the propagation distance in magnetic field.

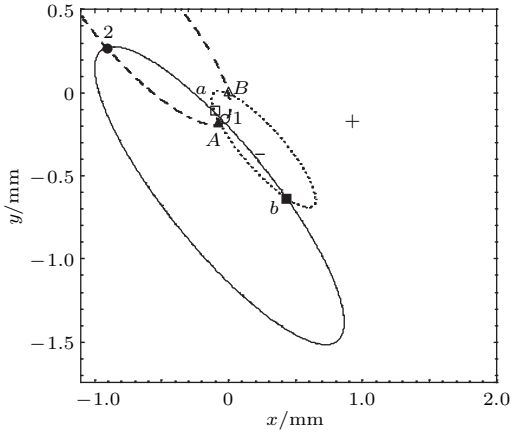

图 4 电场 $s_1=0$, $s_2=0$ 和 $s_3=0$ 的等值线分布图

Fig. 4. Contour lines of $s_1=0$, $s_2=0$ and $s_3=0$ in electric field.

5 结 论

本文基于光谱Stokes参数和复光谱Stokes场, 以刃型位错光束为例, 对傍轴近似下随机电磁光束经像散透镜聚焦后空间的磁场光谱Stokes奇点演化特性进行了讨论, 并与对应随机电磁光束的电场光谱Stokes奇点做了比较. 结果表明, 部分相干刃型位错光束在聚焦空间传输过程中存在着磁场的光谱 s_{12}, s_{23} 和 s_{31} Stokes奇点. 通过改变光束的刃型位错的离轴参数、斜率、部分相关长度等光束控制参数以及传输距离, 会出现磁场光谱 s_{12}, s_{23} 和 s_{31}Stokes奇点的移动、产生和湮没等. 适当改变控制参数或传输距离, 产生和湮没会出现在两拓扑电荷相反的光谱Stokes奇点对之间, 还会出现 V 点和发生 C 点旋向性的反转. 与随机电磁光束电场的光谱Stokes奇点比较表明, 两者位置、旋向性或拓扑电荷等一般不相同, 且左右旋空间也不一致. 本文所得结果深化了对电磁束的偏振奇点变化规律的认识.

参考文献

[1] Nye J F, Hajnal J V 1987 *Proc. R. Soc. Lond. A* **409** 21

[2] Soskin M S, Vasnetsov M V 2001 *Prog. Opt.* **42** 219

[3] Nye J F 1999 *Natural Focusing and the Fine Structure of Light* (UK: IOP Publishing, Bristol) pp373–381

[4] Berry M V, Dennis M R 2001 *Proc. R. Soc. Lond. A* **457** 141

[5] Konukhov A I, Melnikov L A 2001 *J. Opt. B* **3** S139

[6] Freund I 2001 *Opt. Lett.* **26** 1996

[7] Freund I 2002 *Opt. Commun.* **201** 251

[8] Mokhun A I, Soskin M S, Freund I 2002 *Opt. Lett.* **27** 995

[9] Freund I, Mokhun A I, Soskin M S, Angelsky O V, Mokhun I I 2002 *Opt. Lett.* **27** 545

[10] Angelsky O, Mokhun A, Mokhun I, Soskin M 2002 *Opt. Commun.* **207** 57

[11] Angelsky O V, Mokhum I I, Mokhum A I 2002 *Phys. Rev. E* **65** 036602

[12] Soskin M S, Denisenko V, Freund I 2003 *Opt. Lett.* **28** 1475

[13] Flossmann F, Schwarz U T, Maier M, Dennis M R 2005 *Phys. Rev. Lett.* **95** 253901

[14] Schoonover R W, Visser T D 2006 *Opt. Express* **14** 5733

[15] Dennis M R 2008 *Opt. Lett.* **33** 2572

[16] Felde C V, Chernyshov A A, Bogatyryova G V, Polyanskii P V, Soskin M S 2008 *JETP Lett.* **88** 418

[17] Chernyshov A A, Felde C V, Bogatyryova H V, Polyanskii P V, Soskin M S 2009 *J. Opt. A: Pure Appl. Opt.* **11** 094010

[18] Yan H, Lü B 2009 *Opt. Lett.* **34** 1933

[19] Soskin M S, Denisenko V G, Egorov R I 2004 *Proc. of SPIE* **5458** 79

[20] Bliokh K Y, Niv A, Kleiner V 2008 *Opt. Express* **16** 695

[21] Korotkova O, Wolf E 2005 *Opt. Lett.* **30** 198

[22] Luo Y M, Lü B D 2010 *J. Opt.* **12** 115703

[23] Hajnal J V 1990 *Proc. R. Soc. Lond. A* **430** 413

[24] Berry M V 2004 *J. Opt. A: Pure Appl. Opt.* **6** 475

[25] Luo Y M, Lü B D, Tang B H, Zhu Y 2012 *Acta Phys. Sin.* **61** 134202 (in Chinese) [罗亚梅, 吕百达, 唐碧华, 朱渊 2012 物理学报 **61** 134202]

[26] Luo Y M, Gao Z H, Tang B H, Lü B D 2013 *J. Opt. Soc. Am. A* **30** 1646

[27] Liu L H, Lü W Y, Yang C, Mai C J, Chen D P 2015 *Acta Phys. Sin.* **64** 034208 (in Chinese) [刘李辉, 吕炜煜, 杨超, 麦灿基, 陈德鹏 2015 物理学报 **64** 034208]

[28] Wolf E 2007 *Introduction to the Theory of Coherence and Polarization of Light* (Cambridge: Cambridge University Press) pp174–201

[29] Freund I, Shvartsman N 1994 *Phys. Rev. A* **50** 5164

Magnetic spectral Stokes singularities of stochastic electromagnetic beams through an astigmatic lens*

Zheng Shang-Bin[1)] Tang Bi-Hua[1)] Jiang Yun-Hai[1)] Gao Zeng-Hui[2)] Luo Ya-Mei[1)2)†]

1) (*School of Medical Information and Engineering, Southwest Medical University, Luzhou 646000, China*)

2) (*Key Laboratory of Computational Physics, Yibin University, Yibin 644000, China*)

(Received 16 May 2016; revised manuscript received 8 September 2016)

Abstract

Much interest has been aroused in the polarization singularities. A new technique for metrology called singular Stokes polarimetry based on the detection of polarization singularities has been recently developed and used to detect deformations and displacements of samples on a submicron scale, to measure the topology of polarized speckle field and to study the biomedicine as well. The polarization singularities have been extensively studied theoretically, numerically and experimentally. However, most of the studiesare restricted within the frameworks of the fully coherent wave-fields. By using the spectral Stokes parameters introduced by Korotkova and Wolf [Korotkova O, Wolf E 2005 *Opt. Lett.* **30** 198], Yan and Lü [Yan H, Lü B 2009 *Opt. Lett.* **34** 1933] have extended the concept of the polarization singularities from fully coherent beams to partially coherent beams. On the other hand, Hajnal [Hajnal J V 1990 *Proc. R. Soc. Lond. A* **430** 413] studied the electric and magnetic polarization singularities in free-space propagation experimentally with microwaves and confirmed that the electric and magnetic polarization singularities are not coincident in general.

In this paper, taking the partially coherent edge dislocation beam for example, the explicit magnetic propagation expression for stochastic electromagnetic beam through an astigmatic lens is derived based on the representation of cross-spectral density matrix propagation. Using the spectral Stokes parameters the magnetic spectral singularities are studied in detail. It is shown that there exist magnetic spectral s_{12}, s_{23} and s_{31} singularities of stochastic electromagnetic beams through an astigmatic lens. The magnetic spectral Stokes singularities correspond to the zero points of complex Stokes fields $s_{ij} = 0$. s_{12} singularity corresponds to the circular polarization (C-point) of partially coherent beam, and $s_3 > 0$ ($s_3 < 0$) means right- (left-) handedness, where the orientations of the major and minor axes of the polarization ellipse become undefined. s_{23} and s_{31} singularities must be located on L-lines, where the handedness of the polarization ellipse is undetermined (linear polarization). By suitably varying a control parameter, such as off-axis distance, slope of edge dislocation, spatial correlation length, and astigmatic coefficient or propagation distance, the motion, creation, and annihilation of magnetic spectral Stokes singularities may appear. It has been shown that a pair of C-points with equal but opposite topological charges and with similar handedness may be created or annihilated. The V point and handedness reversal of C point may take place. Compared with the electric spectral Stokes singularities of stochastic electromagnetic beams, the positions are not the same, and the left- and right-handedness spaces do not coincide. The results obtained in this paper would be useful for an in-depth understanding of polarization singularities of stochastic electromagnetic beams.

Keywords: stochastic electromagnetic beam, through an astigmatic lens, magnetic spectral Stokes singularity

PACS: 42.25.Bs, 42.25.Ja **DOI:** 10.7498/aps.65.234201

* Project supported by the National Natural Science Foundation of China (Grant Nos. 61275203, 61505075) and the Natural Science Foundation of the Education Department of Sichuan Province, China (Grant No. 15CZ0017).

† Corresponding author. E-mail: luoluoeryan@126.com